A Study on Performance Analysis of the Helically Coiled Evaporator with Circular Minichannels

Ju-Won Kim
Air-conditioning Division, Digital Appliance Company, LG Electronics, 76, Seongsan, Changwon, Gyeongnam 641-713, Korea
Yong-Bin Im
Deptartment of Refrigeration and Air Conditioning Engineering, Pukyong National University, San 100, Yongdang dong, Nam-gu, Pusan 608-737, Korea
Jong-Soo Kim*
School of Mechanical Engineering, Pukyong National University, San 100, Yongdang dong, Nam-gu, Pusan 608-737, Korea

In order to develop a compact evaporator, experiments that show characteristics of evaporating heat transfer and pressure drop in the helically coiled minichannel were performed in our previous research. This study was focused on the performance analysis of helically coiled heat exchangers with circular minichannels with an inner diameter=1.0 mm. The working fluid was R-22, and the properties of R-22 were estimated using the REFPROP program. Numerical simulation was performed to compare results with the experimental results of the helically coiled heat exchanger. As the heat transfer rate and pressure drop were calculated at the micro segment of the branch channels, the performance of the evaporator was evaluated. The following conclusions were obtained through the numerical simulations of the helically coiled heat exchanger. It showed good performance when the flow rate of each branch channels was suitable to heat load of air-side. The numerical simulation value agreed with experimental results within ±15%. In this study, a numerical simulation program was developed to estimate the performance of a helically coiled evaporator. And, an optimum helically coiled minichannels evaporator was designed

Key Words : Helical Coil, Compact, Evaporator, Heat Transfer, Pressure Drop

Nomenclature

A : Area (m^2)
Bo : Boiling number
c_p : Specific heat (kJ/kg K)
d : Diameter (m)
D : Curvature diameter (m)
De : Dean number ($0.5\mathrm{Re}\sqrt{d_i/D}$)
f : Friction factor
G : Mass velocity (kg/m^2 s)
h : Heat transfer coefficient (W/m^2 K)
i : Specific enthalpy (kJ/kg)
k : Thermal conductivity (W/m K)
L : Length (m)
m : Mass flow rate (kg/h)
Nu : Nusselt number
P : Pressure (kPa)
Pr : Prandtl number
Q : Heat transfer rate (kW)
Re : Reynolds number
T : Temperature (K)
v : Velocity (m/s)
x : Quality

* Corresponding Author,
E-mail : jskim@pknu.ac.kr
TEL : +82-51-620-1502; **FAX** : +82-51-611-6368
School of Mechanical Engineering, Pukyong National University, San 100, Yongdang dong, Nam-gu, Pusan 608-737, Korea. (Manuscript **Received** August 25, 2005; **Revised** April 3, 2006)

Greek symbols

δ : $=D/d_i$
α : Void fraction
ρ : Density (kg/m^3)
υ_{fg} : Specific volume ($\upsilon_g - \upsilon_f$)
μ : Viscosity (Ns/m^2)
Xtt: Lockhart-Martinelli parameter
ω : humidity ratio (kg/kgDA)

Subscripts

a : Air
do : Dry-out
fd : Fully developed
fo : Liquid single phase
g : Gas
hc : Helically coiled channel
i : Inlet
l : Liquid
m : Mean, column number
n : Segment number
o : Outlet
r : Refrigerant
st : Straight channel
TP: Two-phase
w : Wall

1. Introduction

It has been promoted that a minichannel and microchannel saves energy and overcomes space restriction through the high performance and compactness of the heat exchanger, which is a main part of air conditioning and refrigeration systems (Mishima et al., 1993; Kim and Katsuta, 1995; Chaobin et al., 2001). The multi-pass heat exchanger has been used for automobile air conditioning systems because of the high performance and compactness. This heat exchanger used for room air conditioner, has the advantages of reducing charging refrigerant, reducing production cost and is expected to improve heat transfer performance. (Wilmarth and Ishii, 1994) But, generally, at the multi-pass branch channel (Reimann and Seeger, 1986; Kim, 1993) of a header type heat exchanger, refrigerant flow distribution originates unequally at each branch channel. So, at the branch channels the liquid phase has been greatly distributed. It didn't all evaporate and partially remained in the normal liquid state. So, the unequal heat transfer rate of each branch channel is linked to a primary factor, which decreases the ability of the evaporator. To get the highest heat transfer rate for the evaporator, the distribution head is designed to match the heat load of each branch channel. The impact factors of two-phase flow are various in multi-pass channels; these are main channel diameter and branch channel diameter of geometric shape, flow direction, post to which branch channel has been attached, branch channel pitch, refrigerant circulation quantity, quality of header inlet, heat load of branch channel, heat load distribution and so on. But how these factors decide flow distribution of two-phase is hardly explained. In fact, it isn't even known what kinds of characteristics unequal distribution takes on. The best design condition is required for multi-pass branch evaporator of header shape. So, we quantitatively should clarify factors that affect flow distribution and organization, which decides flow distribution. In this study, we analyzed the heat transfer and pressure drop properties of multi-pass type helically coiled evaporator in order to apply to room air conditioning system. By comparing the fundamental study and experimental results about helically coiled channel and evaporator with calculation result through performance projection program, we discussed the best design for multi-pass type helically coiled evaporator.

2. Numerical analysis

2.1 Theoretical model

For performance prediction and the optimum design of helically coiled evaporators, a simulation was performed calculating the heat transfer rate and pressure drop. We divided refrigerant flow channel and air channel by each column (Fig. 1).

Micro segment partition is two-dimensional (m, n) matrix. **m** corresponds the column of the refrigerant and airside and **n** refers to the micro segments (Fig. 2). In theory, helically coiled minichannel to straight channel for 50 parts micro seg-

ment, and using refrigerant condition (heat transfer rate, quality, pressure drop) and air conditions (temperature, humidity, heat transfer rate of airside) from refrigerant and heat balance of airside. The helically coiled evaporator was modeled on 3 column 25 branch channels. After each column was representatively calculated, the branch channel number of each column was multiplied and was calculated with regards to pressure drop and entire heat transfer rate of heat exchanger.

Input data were shape, structure of helically coiled minichannel, mass velocity, evaporating

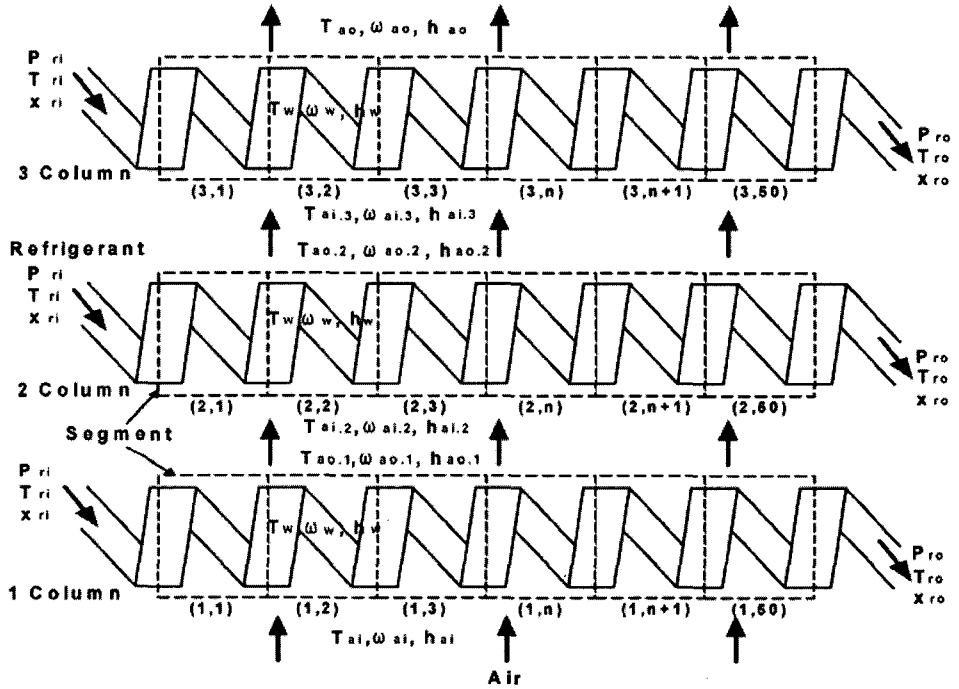

Fig. 1 Detailed arrangement of helically coiled evaporator

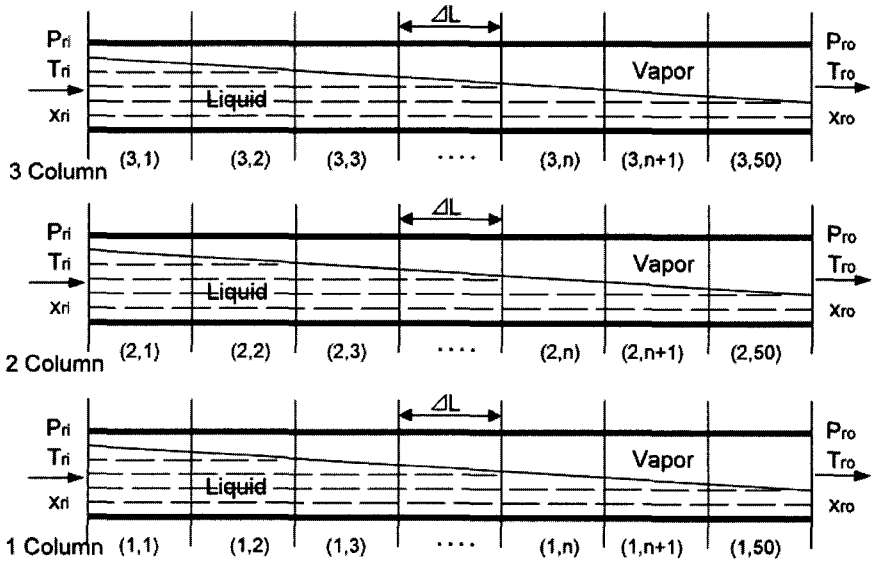

Fig. 2 Model of refrigerant flow

Table 1 Dimension of helically coiled heat exchanger

	Dimension
Inner diameter (mm)	1.0
Straight length (mm)	1500
Pitch of column (mm)	11
Pitch of row (mm)	5.5
Branch channels	3×25

temperature, pressure, inlet quality, inlet air temperature, humidity, and velocity distribution of airside.

To compare with experimental results of existing helically coiled evaporator, input data of the simulation was the same as the conditions of the experiment. The dimension of the helically coiled minichannel and the heat exchanger is shown in Table 1. Heat transfer areas are calculated by the interior and exterior channel surface of each micro segment. Air velocity is controlled by core velocity except in the areas of helically coiled minichannel in each micro segment. Refrigerant properties of R-22 standardized REFPROP 5.0 (Gallagher et al., 2000) developed in NIST.

For numerical simulation, the important factors remained unchanged according to time on the assumption of steady state. Oil mixed in the refrigerant isn't considered to have an effect on heat transfer and pressure drop. The efficiency prediction program of helically coiled evaporators was divided into two parts. Part one's included minichannel decay, and refrigerant side and airside entrance conditions. The basic equation, pressure drop, heat transfer rate of airside and refrigerant side were calculated in part two. First, initial heat flux and temperature of wall surface are assumed to calculate the program. Therefore, it calculates the void fraction, velocity and two phase viscosity for refrigerant R-22, Re and Bo numbers are needed for heat transfer and pressure drop calculation.

The pressure drop is calculated as a two-phase flow friction factor for straight channels. And, the friction factor is calculated with regards to the helically coiled minichannel, friction loss and acceleration loss is calculated with regards to infinitesimal sections and each pressure drop in the infinitesimal section is estimated synthetically by the pressure drop of entire evaporator. A part heat transfer rate of each micro segment calculates in the heat exchange rate of the evaporator. The heat exchange rate of micro segment is calculated by assuming the temperature of the wall surface. And, the heat exchange rate of airside is calculated by enthalpy and humidity ratio. The heat exchange rate of refrigerant side and airside are compared until error agrees within ±5%. So, the temperature of the wall surface was calculated repeatedly.

2.2 Numerical procedure

When a helically coiled minichannel is spread by the straight channel (Fig. 2), mass equation, momentum equation and energy balance equation can be shown as a general equation between cross section 1 of micro segment (1,1) and across section 2 of micro segment (1,2). Mass flux and the velocity of gas and liquid were calculated by using quality and Smith's void fraction. (Smith, 1969)

$$\dot{m}_l=\dot{m}(1-x),\ \dot{v}_l=\dot{m}/[\rho_f(1-\beta)],\quad \dot{m}_g=\dot{m}x,\ v_g=m/[\rho_g\beta A] \tag{1}$$

The friction factor of the single phase flow of helically coiled minichannels can use the correlative Eq. (2) of Prandtl that was suggested by revising relative Eq. about straight channels during the fundamental experiment. Also, calculation of friction factor in two phase flow was used Eq. (3) of helically coiled minichannels that were adjusted through Ito's correlative Eq. (9)

$$f_{hc}=f_{st}\times 0.37(De)^{0.36},\ \frac{10^{1.6}}{2}<De<500 \tag{2}$$

$$f_{hc.TP}=f_{TP}\left[\mathrm{Re}\left(\frac{d_i}{D}\right)^2\right]^{1/20},\ \mathrm{Re}\left(\frac{d_i}{D}\right)^2>6 \tag{3}$$

The Eq. (3) of two phase flow about straight channel used correlative Eq. (4) of Blasius and viscosity of two phase flow used viscosity Eq. (5) of Dukler.

$$f_{TP}=0.079[Gd_i/\mu_{TP}]^{-1/4} \tag{4}$$

$$\mu_{TP}=\rho_{TP}[xv_g\mu_g+(1-x)v_l\mu_l] \tag{5}$$

Pressure drop of the helically coiled minichannels causes pressure drop of friction. Therefore friction loss and acceleration loss were calculated by using Eq. (6), and pressure loss for gravity was ignored. Also, pressure drop of the distribution header was not calculated. The pressure drop was calculated from inlet to outlet of generating channel.

$$\Delta P=\frac{2f_{hc,TP}LG^2v_f}{d_i}\left[1+\frac{x}{2}\left(\frac{v_{fg}}{v_f}\right)\right]+G^2v_f\left(\frac{v_{fg}}{v_f}\right)x \tag{6}$$

To calculate the heat transfer coefficient of inside the channel, the heat transfer correlation of Schrock-Grossman's (Tatshiro, 1989) nuclear boiling and forced convection evaporation were used, heat transfer coefficient for liquid single-phase of helically coiled channel was estimated with the equation that was suggested in previous research (Kim et al., 2002) on helically coiled channel.

$$\frac{h_{TP}}{h_{fo}}=0.739\left[Bo\times10^4+1.5\left(\frac{1}{X_{tt}}\right)^{2/3}\right] \tag{7}$$

$$Nu_{fd}=\{0.09+0.01(1+0.8\delta^{-0.9})\}\Pr^{1/3}\mathrm{Re}^m\left(\frac{\Pr}{\Pr_w}\right)^{0.14}$$
$$m=0.5+0.2903\delta^{-0.194},\ \delta=\frac{D}{d_i} \tag{8}$$

After dry-out, heat transfer coefficient for single-phase of refrigerant vapor was estimated with the empiric formula of Kays. (Kays and Crawford, 1993)

$$h_g=0.021\frac{k_g}{d_i}\left(\frac{Gd_i}{\mu_g}\right)^{0.8}\left(\frac{c_{pg}\mu_g}{k_g}\right)^{0.5} \tag{9}$$

If the channel diameter was smaller, it was found that the quality for the beginning degradation of heat transfer rate was advanced (Kim et al., 2002). These researching results were reported. (Shizuo et al., 2000; Kim et al., 2001) In this simulation, the quality for generation of dry-out fixed 0.6 through the basic research findings of helically coiled channel. After dry-out, heat transfer coefficient was obtained by Eq. (10) using the evaporation heat transfer coefficient and vapor single-phase heat transfer.

$$h_{do}=h_{TP}\sin^2\left[\frac{\pi(1-\varepsilon)}{2}\right]+h_g\cosh^2\left[\frac{\pi(1-\varepsilon)}{2}\right],\quad \varepsilon=(x-x_{do})/(1-x_{do}) \tag{10}$$

In view of getting done simultaneously sensible and latent heat exchange on the outside of helically coiled channel, airside heat transfer coefficient of enthalpy basis can be represented by experimental equation. (Tatshiro, 1989) Airside heat transfer coefficient can be represented by function of air velocity as follows.

$$h_a=141.4v_m^{0.86} \tag{11}$$

The air is saturated on the evaporator wall and the humidity ratio can be calculated by Eq. (12), (13).

$$\omega_w=0.622\frac{P_s}{(P_a-P_s)} \tag{12}$$

$$P_s=\exp\left[18.3036-\frac{3816.44}{(T_w-46.13)}\right] \tag{13}$$

Enthalpy of air is calculated by temperature and humidity ratio.

$$i=\frac{c_{pa}(T_a-273.15)}{1+\omega_a}+\frac{[597.3+c_{va}(T_a-273.15)]\omega_a}{1+\omega_a} \tag{14}$$

Outlet humidity ratio of micro segment on airside in Fig. 1 is calculated by Eq. (15). Outlet Temperature on airside can be calculated by the same method.

$$\omega_o=\frac{(\omega_i-\omega_w)}{(i_i-i_w)}(i_o-i_w)+\omega_w \tag{15}$$

If the wall temperature is assumed for the performance evaluation, heat exchange rate of refrigeration can be calculated by Eq. (16).

$$Q_r=h_rA(T_w-T_b) \tag{16}$$

On the assumption that the wall temperature can be calculated by enthalpy, heat exchange rate on airside and enthalpy of outlet are calculated by following Eq. (17) and (18) with simultaneous equations. The wall temperature calculation is repeated until a point of agreement between heat transfer rate of refrigerant side and that of airside

is achieved.

$$Q_a = G_a A (i_i - i_o) \tag{17}$$

$$Q_a = h_a A (i_i - i_o) / \ln \frac{i_i - i_w}{i_o - i_w} \tag{18}$$

When heat exchange rate on airside and refrigerant side is the same, heat exchange rate, air temperature of outlet and outlet quality of refrigerant are calculated. Also, the quality of the micro segment is calculated by Eq. (19) using latent heat of vaporization in refrigerant heat transfer rate on airside.

$$\Delta x = \frac{Q_a}{\dot{m}_r \Delta i} \tag{19}$$

Heat exchange rate of branch channels can be summed as the heat exchange rate of each micro section. When calculation of the first column is finished, Fig. 1 represents the outlet air condition of the first column and sets up the inlet air condition of second column, calculating total heat exchange rate and pressure drop. The third column is calculated by the same method to discover the entire heat exchange rate of helically coiled evaporators. The thermal load on the air side of helically coiled evaporators is different from each column. Inlet air temperature of each column is lower, as the third column extends. Because thermal load on airside is decreased, the proper flow distribution is realized in the thermal load of each line on airside. So, the optimum ability of helically coiled evaporator makes manifest.

For seeking the best heat exchange rate of the evaporator in the performance calculation, performance of the helically coiled evaporator is calculated by identifying refrigerant flow and controlling refrigerant flow of Eq. (19), when outlet superheat is around 5℃.

3. Results and Discussion

The input simulation conditions are used to compare calculation results with experimental results. These conditions are shown in Table 2. Other conditions were used with the same mass and air velocity with the test of the helically coiled evaporator. It was calculated for heat transfer rate, outlet air temperature and humidity ratio on the air side, and heat transfer rate, pressure drop and outlet quality on the refrigerant side.

3.1 Heat transfer rate and pressure drop

The heat transfer rate of the simulation result and the experimental value in helically coiled evaporator is compared in Fig. 3 for the same input conditions; evaporating temperature=5℃, inlet quality=0.2, inlet air temperature=27℃ and inlet humidity ratio=0.01115 kg/kgDA. The heat transfer rate in the experimental results is about 1.6 kW at 1 m/s and 2.4 kW at 1.5 m/s. When heat transfer rate in the simulation result was compared with the experimental result, it was confirmed within ±15%. The heat transfer rate of one branch channel for each column is shown in Fig. 4. When the refrigerant mass velocity is the same for each channel, the heat transfer rate shows a tendency to decrease marginally.

Table 2 Simulation conditions

No	Refrigerant mass velocity (kg/m^2s)	Air velocity (m/s)
1	150	1
2		1.5
3	200	1
4		1.5
5	250	1
6		1.5

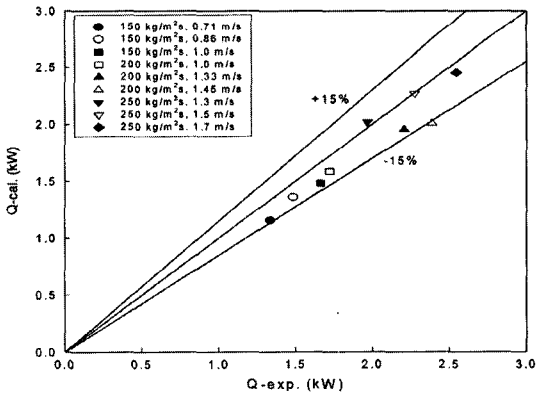

Fig. 3 Comparison of heat transfer rate between experiment and calculation

When the refrigerant mass velocity is controlled as the outlet superheat (5℃) of the branch channels, the heat transfer rate of the first column increased greatly because the heat load of airside is the highest at first column. In Fig. 5, it was compared pressure drop of unit length between experiment and calculation results. The pressure drop between experiment and calculation results is within ±15% under 200 kgm^{2}s. But experimental results are lower than calculation results by about 20~30% over 200 kg/m^{2}s. Calculation results were different from experimental results because pressure drop from pressure measurement point to distribution header and through distribution header was not considered. So, as the mass velocity grew higher, the distribution header grew bigger and the differences between experiment and calculation results increased.

3.2 Local heat transfer coefficient and variation of quality

Figure 6 represents the local heat transfer coefficient of the micro segment that was corresponding quality. In this case, superheat of the branch channel for each column was controlled at 5℃ and the mass velocity was optimum for the heat road of the air side. The first column had the highest local heat transfer coefficient, the second column, then the third.

Figures 7 and 8 represent the variation of quality corresponding to the length of branch channels for each column. When mass velocity flew constantly at 200 kg/m^{2}s, superheat began about 1 m

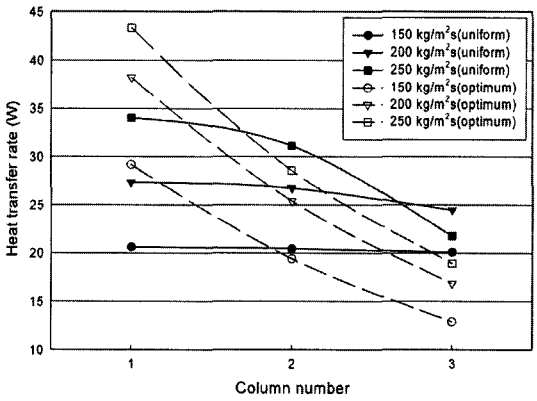

Fig. 4 Comparison of heat transfer rate with column number. (Air velocity : 1.5 m/s)

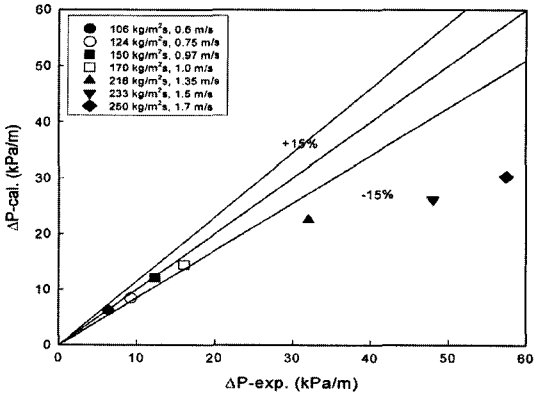

Fig. 5 Comparison of pressure drop between experiment and calculation

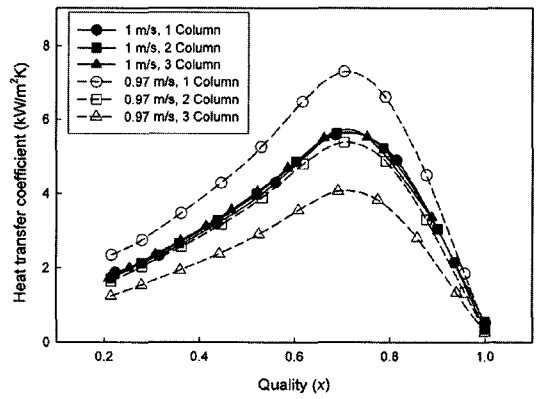

Fig. 6 Comparison of heat transfer coefficient with column number

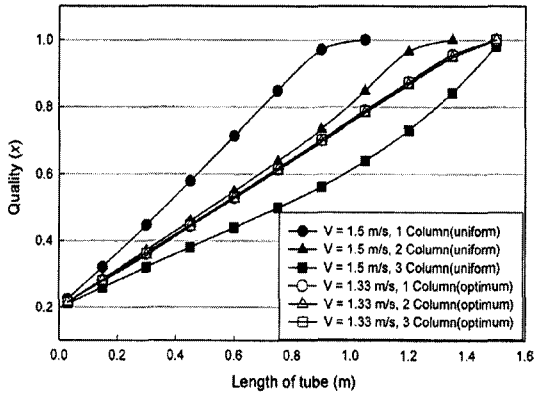

Fig. 7 Quality vs. length of channel

in the first column at about 1.3 m in the second column. In the third column, superheat occurred at the outlet. When mass velocity flew 42~43% more at branch channel of first column, 4~5% in the second column, and decreased 37~38% in the third column. Therefore, outlet superheat of each column was controlled at 5℃. Through, regulating mass velocity of the branch channel for each column, we could obtain equally superheat and the highest heat exchange rate in the helically coiled heat exchanger.

3.3 Superheat

The superheat at the branch channels is represented in Fig. 9. When mass velocity is uniform for each branch channel, superheat is more than 10℃ in the branch channel of first column. In case of 150 kg/m^{2}s and 200 kg/m^{2}s, superheat exceeds 10℃ at the branch channel of the second column. If mass and air velocity have the optimum condition, we could obtain the equal outlet superheat of branch channel for each column.

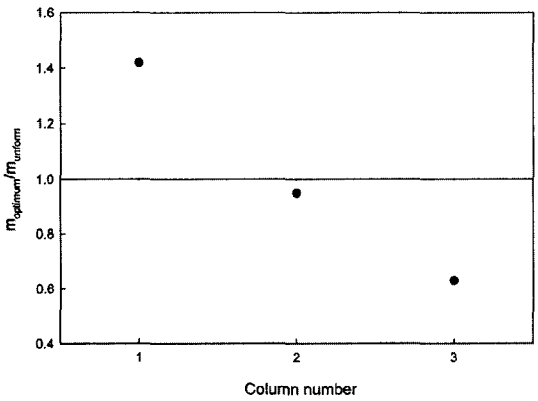

Fig. 8 Comparison of optimum mass velocity with row number

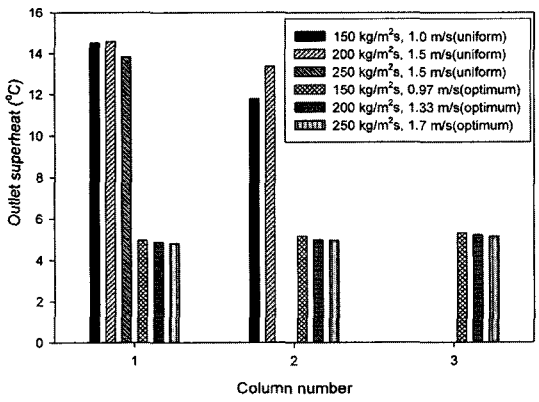

Fig. 9 Comparison of outlet superheat with column number

4. Conclusions

The following conclusions were obtained through a performance analysis of the helically coiled heat exchanger with circular minichannels.

(1) In this study, a numerical simulation program was developed to estimate the performance of the helically coiled evaporator. This program confirmed the accuracy and reliability from the comparisons with the experimental results.

(2) When heat transfer rate was compared between the simulation results and the experimental results, it was confirmed within ±15%. The experiment and calculation results of pressure drop were united in low mass velocity range within ±15%, but due to the pressure drop of the distribution header, those results were different in the high mass velocity range.

(3) Maintaining the outlet superheat at 5℃ to fit mass velocity and inlet air velocity of the branch channel for each column, we acquired the optimized heat exchanger.

(4) By increasing mass velocity flowing in the branch channel of the first column by 40%, 5% in the second column, and decreasing flow by 35% in the third column, we could obtain the appropriate refrigerant distribution for heat load of air side, and optimize the performance of the helically coiled evaporator.

Acknowledgments

This work is supported financially by Korea Science and Engineering Foundation through the Centre For Advanced Environmentally Friendly Energy Systems, Pukyong National University, Korea (Project number: R12-2003-001-01001-0) and Korea Energy Management Corporation under contract number 1997-E-ID01-P-53.

References

Chaobin, D., Hirofumi, D., Eiji, H. and Masahide, T., 2001, "Finned Small Diameter Tube Heat Exchanger," *Trans. of the JSRAE*, Vol. 18, No. 2, pp. 143~151.

Gallagher, J., McLinden, M., Morrison, G. and Huber, M., 2000, "NIST Thermodynamic Properties and Refrigerant Mixtures Database (REFPROP Version 5.0)," *National Institute of Standards and Technology*, Gaithersburg, MD, U.S.A

Kays, W. M. and Crawford, M. E., 1993, "Convective Heat and Mass Transfer," *McGraw-Hill Book*, New York, 3rd ed., p. 324.

Kim, J. S. and Katsuta, M., 1995, "Development of High Performance Heat Exchanger for CFC Alternative Refrigerants (1st Report: Condensing Heat Transfer and Pressure Drop of HFC-134a in Multi-Pass Tubes)," *J. Refrigeration Engineering & Air Conditioning*, Vol. 14, No. 5, pp. 273~283.

Kim, J. S., 1993, "Two Phase Flow Distribution in Multi-Parrallel Evaporator Tubes (1st Report: Non-Heating Mode)," *Journal of Refrigeration & Air Conditioning Engineering*, Vol. 12, No. 1, pp. 9~19.

Kim, J. W., Kim, J. H., Seo, S. K., Kim, J. H. and Kim, J. S., 2002, "Characteristics of Heat Transfer and Pressure Drop of R-22 Inside an Evaporating Tube with Small Diameter Hellical Coil," *Transactions of the Korean Society of Mechanical Engineers B*, Vol. 24, No. 5, pp. 699~708.

Kim, J. W., Kim, J. H. and Kim, J. S., 2001, "A Study on the Helically Coiled Heat Exchanger of Small Diameter Tubes," *Transactions of the Korean Society of Mechanical Engineers, B*, Vol. 25, No. 11, pp. 1492~1499.

Mishima, K., Hibiki, T. and Nishihara, H., 1993, "Some Characteristics of Gas-liquid Flow in Narrow Rectangular Ducts," *Int. J. Multiphase Flow*, Vol. 19, No. 1, pp. 115~124.

Oh, H. K., Katsuta, M. and Shibata, K., 1998, "Heat Transfer 1998," *Proc. 11th IHTC*, Korea, Vol. 6, pp. 131~136.

Reimann, J. and Seeger, W., 1986, "Two Phase Flow in a T-Junction with Horizontal Inlet, Part 2: Pressure Difference," *Int. J. Multiphase Flow*, Vol. 12, No. 4.

Shizuo, S., Hirofumi, D. and Eiji, H., 2000, "Study on Boiling Heat Transfer of Refrigerants inside Horizontal Micro Tubes," *37th National Heat Transfer Symposium of Japan*, Vol.3, Kobe.

Smith, S. L., 1969, Proc. Instn. Mech. Engrs., Vol. 184, Pt 1. (36), pp. 647~657.

Tatshiro, U., 1989, "Gas-liquid Two-phase Flow," 2nd ed., pp. 262, Tokyo.

Wilmarth, T. and Ishii, M., 1994, "Two-Phase Flow Regimes in Narrow Rectangular Vertical and Horizontal Channels," *Int. J. Heat Mass Transfer*, Vol. 37, No. 12, pp. 1749~1758.